PRECISION MEASUREMENTS FROM THE NOMAD EXPERIMENT

R. PETTI
CERN, CH-1211 Genéve 23, Switzerland
E-mail: Roberto.Petti@cern.ch
(for the NOMAD collaboration)

The NOMAD experiment collected unprecedent neutrino data samples, matching both the large statistics of massive calorimeters and the reconstruction quality of bubble chambers. This paper describes the determination of the weak mixing angle which is ongoing in NOMAD, with a target precision of $\sim 1\%$. In addition, measurements of the ν_μ quasi-elastic cross-section and of neutrino Charged Current differential cross-section on carbon are presented.

1 Introduction

The NOMAD experiment was designed to search for ν_τ appearance from neutrino oscillations in the CERN wide-band neutrino beam produced by the 450 GeV proton synchrotron. The single-particle reconstruction and lepton identification capability of the NOMAD detector allowed the search for ν_τ appearance in most of the leptonic and hadronic τ decay channels [1] and also to look for $\nu_\mu \rightarrow \nu_e$ oscillations [2]. No evidence for oscillations was found.

A second phase of the NOMAD analysis started after the completion of the oscillation searches, with the aim of exploiting the high quality of the available neutrino data samples for precise measurements of cross-sections and particle production. This activity could benefit from the beam and detector studies performed for the oscillation searches.

2 Detector and data samples

The NOMAD detector is described in detail in Ref. [3]. Inside a 0.4 T magnetic field there is an active target consisting of drift chambers (DC) [4] with a fiducial mass of about 2.7 tons and a low average density (0.1 g/cm^3). The main target, 405 cm long and corresponding to about one radiation length, is followed by a transition radiation detector (TRD) [5] for electron identification, a preshower detector (PRS), and a high resolution lead-glass electromagnetic calorimeter (ECAL) [6]. A hadron calorimeter (HCAL) and two stations of drift chambers for muon detection are located just after the downstream part of the magnet coil. An iron-scintillator sampling calorimeter with a fiducial mass of about 17t (FCAL) is located upstream of the central part of the NOMAD target. The detector is designed to identify leptons and to measure muons, pions, electrons and photons with comparable resolutions. Momenta are measured in the DC with a resolution:

$$\frac{\sigma_p}{p} \simeq \frac{0.05}{\sqrt{L[m]}} \oplus \frac{0.008 \times p[GeV/c]}{\sqrt{L[m]^5}}$$

where L is the track length and p is the momentum. The energy of electromagnetic showers, E, is measured in the ECAL with a resolution:

$$\frac{\sigma_E}{E} = 0.01 \oplus \frac{0.032}{\sqrt{E[GeV]}}.$$

The relative composition of CC events in NOMAD is estimated [7] to be ν_μ,: $\bar{\nu}_\mu$,: ν_e,: $\bar{\nu}_e$ = 1.00 : 0.0227 : 0.0154 : 0.0016, with average neutrino energies of 45.4, 40.8, 57.5, and 51.5 GeV, respectively. Neutrinos are produced at an average distance of 625 m from the detector.

The NOMAD experiment collected data from 1995 to 1998. Most of the running, for a total exposure of 5.1×10^{19} protons on target (pot), was in neutrino mode. This resulted in three distinct data samples, according to

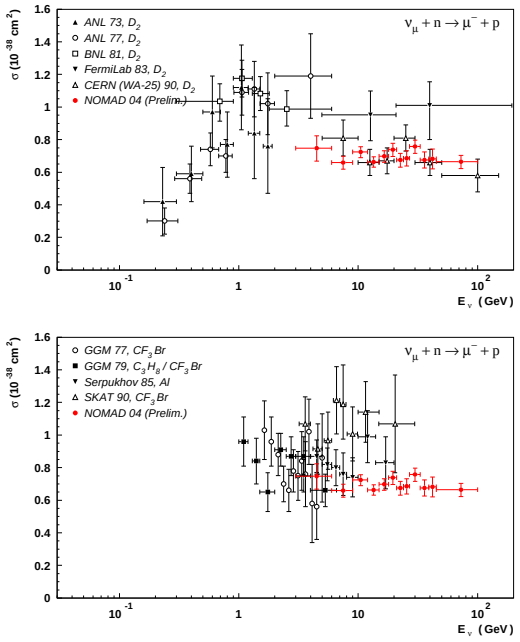

Figure 1. Measurement of the ν_μ quasi-elastic cross-section on carbon in NOMAD (full red circles) compared with all the available data. The upper plot shows results on deuterium targets, while the lower panel results on heavier targets.

the different targets: $1.3 \times 10^6 \nu_\mu$ CC interactions from the drift chambers (mainly carbon), $1.5 \times 10^6 \nu_\mu$ CC interactions from the region of the magnet coil (mainly aluminium) located in front of the DC and $1.2 \times 10^7 \nu_\mu$ CC interactions from FCAL (iron).

3 Precision measurements

3.1 Determination of $\sin^2\theta_W$

A precise determination of the weak mixing angle from νN Deep Inelastic Scattering (DIS) provides a *direct* measurement of neutrino couplings to Z^0, allowing a precision test of Standard Model at a different scale with respect to LEP/SLD. The interest of such measurement increased after the publication of the final results on $\sin^2\theta_W$ by the NuTeV collaboration [8], reporting a deviation of about 3σ with respect to the Standard Model predictions [9].

The NOMAD experiment is extracting the value of $\sin^2\theta_W$ from the ratio of Neutral (NC) to Charged Current ν interactions:

$$\mathcal{R}_\nu = \frac{\sigma_{NC}}{\sigma_{CC}}$$

To reduce systematic uncertainties, a simultaneus fit to both $\mathcal{R}_\nu$ and the CC differential cross-section $d\sigma^2_{CC}/dxdy$ is performed. The analysis consists in classifying the events as NC and CC, providing the experimental ratio $\mathcal{R}_\nu^{\rm exp}$. The knowledge of the detection efficiencies and of the experimental resolutions provides then the cross-section values.

The identification of CC interactions is based upon two *independent* criteria. First, events containing tracks (of any charge) matched to segments in the external muon chambers are flagged as ν_μ CC. A kinematic tagging of the leading lepton is then applied to all events failing the previous requirement. This second tagging is provided by a multi-dimensional likelihood function [1] and is applied to negative tracks only. The procedure provides two substantial advantages. A CC event failing any of the two complemetary criteria has a second possibility to be tagged as CC, thus resulting in a reduction of the corresponding systematic uncertainty by one order of magnitude. In addition, the kinematic tagging is very efficient on electrons from ν_e CC events which are mostly identified without the use of any specific detector requirement. This in turn reduces systematic uncertainties from the ν_e beam content to a negligible level. The fraction of unidentified ν_μ CC events is about 2%.

In principle, the theoretical model enters both in the Monte Carlo simulations used for the efficiency corrections and in the final fit to extract $\sin^2\theta_W$. However, a refined Data Simulator technique [1] is used to extract all efficiencies from the data themselves, for both NC (with a NC-simulator) and CC (with a CC-simulator), through the

Source of uncertainty	$\delta\mathcal{R}_\nu/\mathcal{R}_\nu$
Statistics	0.00207
Experimental systematics	0.00194
Model systematics	0.00181
TOTAL	0.00336

Table 1. Summary of the relative uncertainties for the NOMAD measurement of the NC to CC ratio $\mathcal{R}_\nu$. The numbers refer only to the main data sample from the DC target (carbon).

expression $\epsilon = \epsilon_{\rm MC} \times \epsilon_{\rm DS}/\epsilon_{\rm MCS}$, where $\epsilon_{\rm MC}$, $\epsilon_{\rm DS}$ and $\epsilon_{\rm MCS}$ are the efficiencies extracted from the Monte Carlo, the Data Simulator and the Monte Carlo Simulator. The model largely cancels in the ratio $\epsilon_{\rm MC}/\epsilon_{\rm MCS}$. As a result, experimental efficiencies are stable against changes in the simulations.

A preliminary estimate of the NOMAD sensitivity to $\mathcal{R}_\nu$ is shown in Table 3.1. The dominant constributions to the systematic uncertainty are the determination of the NC trigger efficiency and the knowledge of the strange sea distribution. The corresponding precision on the $\sin^2\theta_W$ extraction is $\sim 1\%$, comparable to NuTeV [8], E158 [15] and APV [16]. It must be noted the addition of the sample of events from the front coil of the NOMAD magnet would reduce both the statistical uncertainty and the experimental systematics since the latter is defined by the size of the control samples from data.

The analysis is "blind" and the value of $\sin^2\theta_W$ will be available only after all the systematic uncertainties are finalized.

3.2 Quasi-elastic $\nu_\mu C$ cross-section

The reconstruction and identification of the recoiling proton track allowed a measurement of the quasi-elastic cross-section $\nu_\mu n \to \mu^- p$ on carbon in NOMAD. A kinematic analysis based upon a three-dimensional likelihood function is used to reject backgrounds from DIS and resonance production. Overall, 8192 events are selected with a signal efficiency of 25% and a purity of 71%. The measurement is performed in the energy range $3 < E_\nu < 100$ GeV.

In order to reduce systematic uncertainties, NOMAD is measuring the *ratios* of quasi-elastic cross-section with respect to two independent processes: DIS ($W^2 > 4$ GeV^2) and Inverse Muon Decay (IMD) $\nu_\mu e^- \to \mu^- \nu_e$. The absolute normalization is provided by the world average cross-section on isoscalar target for DIS and by the theoretical cross-section for IMD. Both measurements are consistent. Figure 1 shows a comparison of the preliminary NOMAD results on carbon with a compilation of existing data.

3.3 Cross-sections and structure functions

The present knowledge of neutrino cross-sections is rather nonuniform. In the region $E_\nu > 30$ GeV, where data from the large massive calorimeters (CCFR, NuTeV) are available, the uncertainty is about 2%. This increases to about 20% at lower energies, due to the limited statistics of bubble chamber experiments. Measurements of both the total $\sigma^{\rm tot}_{CC}$ and the differential $d\sigma^2_{CC}/dxdy$ cross-sections for ν_μ are performed in NOMAD, as part of the $\sin^2\theta_W$ analysis.

The absolute normalization is obtained from the world average cross-section on isoscalar target in the energy range $40 < E_\nu < 300$ GeV. A comparison of the measured differential cross-section on carbon with the model predictions (Sec. 3.5) is shown in Figure 2.

The NOMAD cross-section data are also used to extract the structure functions F_2 and xF_3. The average Q^2 is about 13 GeV^2, with events extending to the few GeV^2 region. In addition, it is possible to study nuclear effects in neutrino structure functions by comparing the results with C, Al and Fe targets.

3.4 Charm production and strange sea

The sample of events (1.2×10^7 ν_μ CC) originating in the forward iron calorimeter is used to measure the charm dimuon production in ν interactions. A total of 12767 ± 205 identified charm events (after background subtraction) is selected, providing the single largest neutrino sample available.

The value of the charm quark mass m_c, the strange sea suppression factor η_s and the semileptonic branching ratio B_μ are extracted from a fit to kinematic distributions obtained from the *ratio* of dimuons to single muon events. Many systematic uncertainties cancel in such ratio. In addition, the energy spectrum of the NOMAD flux [7] provides a good sensitivity to the charm threshold.

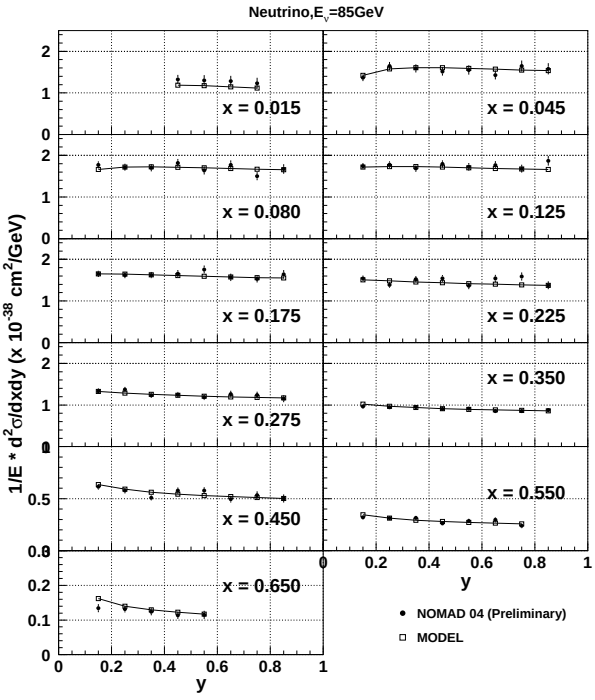

Figure 2. Results from the NOMAD measurement of the ν_μ differential cross-section $d\sigma^2_{CC}/dxdy$ on carbon at $E_\nu = 85$ GeV (full circles). The open squares show the NNLO model predictions (Sec. 3.5), based upon the use of charged lepton scattering data only.

3.5 Modelling

The determination of $\sin^2\theta_W$ from $\mathcal{R}_\nu$ required the development of a refined modelling of neutrino interactions. A NNLO QCD calculation [10] is performed to obtain the neutrino-nucleon structure functions. Dedicated fits to available data from charged lepton scattering on p and D (BCDMS, E665, HERA, JLab, NMC, SLAC) and from (anti)neutrino scattering (NOMAD, NuTeV), are performed to extract parton distributions, high twist terms and the corresponding uncertainties.

A model of nuclear effects on structure functions is included [11]. This has been defined on the basis of charged lepton nuclear data and checked against cross-section data. It includes shadowing, off-shell, Fermi motion and binding energy, pion contributions and non-isoscalarity corrections.

A new evaluation of electroweak radiative corrections to structure functions is also used [12]. Results from an independent calculation [13] allow a cross-check of systematic uncertainties.

A detailed tuning of fragmentation parameters is extracted with the analysis of individual tracks in the hadronic system reconstructed in ν_μ CC data.

The charm production parameters are determined primarily from the analysis of NOMAD dimuon data in FCAL (Sec. 3.4). The mass of the charm quark ($\overline{MS}$ scheme) is further constrained by data from production thresold in e^+e^- collisions [14]. A precise parameterization of the strange sea distribution is obtained by including NOMAD dimuon data in the global fits to extract parton distributions.

References

1. P. Astier et al. *Nucl. Phys.* **B** 611, 3 (2001).
2. P. Astier et al. *Phys. Lett.* **B** 570, 19 (2003).

3. J. Altegoer et al. *Nucl. Instr. and Meth.* **A** 404, 96 (1998).
4. M. Anfreville et al. *Nucl. Instr. and Meth.* **A** 481, 339 (2002).
5. G. Bassompierre et al. *Nucl. Instr. and Meth.* **A** 403, 363 (1998); G. Bassompierre et al. *Nucl. Instr. and Meth.* **A** 411, 63 (1998).
6. D. Autiero et al. *Nucl. Instr. and Meth.* **A** 372, 556 (1996); D. Autiero et al. *Nucl. Instr. and Meth.* **A** 373, 358 (1996); D. Autiero et al. *Nucl. Instr. and Meth.* **A** 387, 352 (1997); D. Autiero et al. *Nucl. Instr. and Meth.* **A** 411, 285 (1998); D. Autiero et al. *Nucl. Instr. and Meth.* **A** 425, 188 (1999).
7. P. Astier et al. *Nucl. Instr. and Meth.* **A** 515, 800 (2003).
8. G. Zeller et al. *Phys.Rev.Lett.* 88, 091802 (2002).
9. S. Davidson, S. Forte, P. Gambino, N. Rius and A. Strumia, hep-ph/0112302; W. Melnitchouk and A. Thomas, hep-ex/0208016; S. Kulagin, hep-ph/0301045; K. McFarland and S. Moch, hep-ph/0306052; B. Dobrescu and R. Ellis, hep-ph/0310154.
10. S. Alekhin, *Phys. Rev.* **D** 67, 114002 (2003).
11. S. Kulagin and R. Petti, *paper in preparation.*
12. A. Arbuzov, D. Bardin and L. Kalinovskaya, hep-ph/0407203.
13. K. Diener, S. Dittmaier and W. Hollik, hep-ph/0310364.
14. J. Kuhn and M. Steinhauser, hep-ph/0109084.
15. R. McKeown, these proceedings.
16. C. Wood et al., Science 275 (1997) 1759.